EuroGNC Navigation Guidance Control CEAS Bristol, UK June 11th-13th 2024
University of BRISTOL ROYAL AERONAUTICAL SOCIETY AIAA

Steep Descent Control Algorithm for Shipborne Sea-Skimming Missiles

Tuna Gün Aksu Middle East Technical University, Aerospace Engineering Department & Specialist Design Engineer, ROKETSAN, Cruise Missile Systems, 06780, Ankara, Turkiye. tuna.aksu@roketsan.com.tr

Özgün Dülgar Lead Design Engineer, ROKETSAN, Cruise Missile Systems, 06780, Ankara, Turkiye. ozgun.dulgar@roketsan.com.tr

Halil Ersin Söken Assoc. Prof. Dr., Middle East Technical University, Department of Aerospace Engineering, 06800, Ankara, Turkiye. esoken@metu.edu.tr

ABSTRACT

Sea-skimming missiles are missiles which fly very close to sea surface. This is to avoid detection by radar or make it difficult for defense systems to intercept the missile. Sea-skimming missiles are expected to descend to the surface of the water to start avoiding detection as early as possible right after launch. However, this steep descent is a challenging task because of the platform movements, ballistic phase with the booster, and different environmental conditions. It is also expected that the missile's descent should be fast without any overshoot because of the sea below. Thus, a robust and rapid descent control system is one of the main challenges for sea-skimming missiles. The present study proposes modified proportional-derivative controller with predictive model for calculating the system input for the powered descent to the sea surface, with no or minimum overshoot. The effectiveness of the proposed method is evaluated through extensive simulations and compared against traditional control approaches. Results for various different scenarios, which include booster thrust vector misalignment, different launch and environmental conditions, are investigated to test the robustness of the proposed algorithm.

Keywords: Sea-Skimming Guidance; Shipborne; Robust Altitude Control; Steep Descent; Predictive Model

Nomenclature

m	=	mass
I_{yy}	=	moment of inertia about body y-axis
l_{ref}	=	reference length
S_{ref}	=	reference area
T, T_0	=	temperature, sea-level temperature
h, h_0	=	height, initial height
v, v_0	=	velocity, initial velocity
a, a_0	=	acceleration, initial acceleration
a_z	=	acceleration in z-axis of missile body frame
θ, θ_0	=	pitch angle, initial pitch angle

Except where otherwise noted, content of this paper is licensed under a Creative Commons Attribution 4.0 International License.

The reproduction and distribution with attribution of the entire paper or of individual pages, in electronic or printed form, including some materials under non-CC-BY 4.0 licenses is hereby granted by the respective copyright owners.

θ_b = booster misalignment angle
α = angle of attack
γ = flight path angle
δ = deflection of control surface
$\vec{V}$ = velocity vector
Q = dynamic pressure
C_x = body x-axis aerodynamic coefficient
C_z = body z-axis aerodynamic coefficient
C_m = pitching moment coefficient
F^b_{aero} = aerodynamic force in missile body frame
M^b_{aero} = aerodynamic moment in missile body frame
t_p = predicted time at pullout
ω_n = natural frequency
ζ = damping ratio
h_{com} = altitude command
$\mathrm{d}t$ = time step

1 Introduction

Sea-skimming missiles play a crucial role in modern warfare. These missiles are specifically designed to fly at extremely low altitudes, skimming the surface of the water, with the primary objective of avoiding radar detection and thwarting interception by defense systems. The ability to descend rapidly and smoothly to the sea surface poses a significant challenge for sea-skimming missiles due to various factors, including platform movements, ballistic phases with boosters, and varying environmental conditions. The steep descent of sea-skimming missiles is a critical maneuver that must be executed precisely and efficiently. A swift descent to the sea surface allows the missile to establish a low profile early on, minimizing the time it is susceptible to detection. However, achieving a fast descent without overshooting poses a complex control problem.

In literature, different approaches have been made about control algorithms for sea-skimming missiles. In Ref. [1], an optimal guidance method using LQR (Linear Quadratic Regulator) is implemented, however initial launch and booster phase of the missile is not considered in this study. Ref. [2], proposes full-state feedback controller using Kalman filter (KF) to estimate noisy radar altimeter measurements and uses a similar open-loop model for estimation but same considerations as in Ref. [1] are left out. Also, for inner loop autopilot with altitude control loops, such as attitude and acceleration autopilots, are analyzed [3]. As a result, acceleration autopilot is chosen for the inner loop. Some studies concentrate on flight at sea-skimming level under disturbances such as sea state and sensor noise [4–7]. There are also studies covering determination of the optimum flight altitude under sea wave disturbances [8]. Although, these studies use similar inner autopilot and estimations from acceleration to altitude, concerns about overshoot and booster phase remains. Model predictive control approach is also discussed in recent years for missiles and unmanned aerial vehicle (UAV) as processors are getting powerful. In [9], similar predictive model is used to produce inputs to the system to control altitude of the vehicle by using model predictive control.

Since trajectory shaping is a part of the problem, guidance methods may also provide a solution. Impact angle and path following are topics that surge in attention and popularity. Especially, path-following algorithms are utilized by cruise missiles, anti-ship missiles, and UAVs to follow complex and long routes and avoid obstacles as in [10–12]. Also, impact angle control can be utilized since if the impact vector angle is selected as zero degrees, the missile will approach the target parallel to the

Except where otherwise noted, content of this paper is licensed under a Creative Commons Attribution 4.0 International License.

The reproduction and distribution with attribution of the entire paper or of individual pages, in electronic or printed form, including some materials under non-CC-BY 4.0 licenses is hereby granted by the respective copyright owners.

ground. However, possible solutions using the guidance methods are slower with respect to the PD or the proposed method, as can be seen in [13].

This study aims to address the challenges associated with the steep descent phase of sea-skimming missiles and proposes a modified PD (proportional-derivative) altitude controller with predictive model for calculating the system input required to achieve a powered descent to the sea-skimming altitude level while minimizing or eliminating the overshoot. The effectiveness of the proposed method will be thoroughly evaluated through various scenarios such as encompassing different initial conditions, booster thrust vector misalignment, and environmental conditions. Moreover, its performance will be compared against traditional control approaches that are commonly employed in sea-skimming missile systems. Through the rigorous analysis and comparison of results, this study aims to demonstrate the promising potential of the newly proposed control system in overcoming the hardships of steep descent for sea-skimming missiles.

The remainder of this paper is organized as follows. Firstly, the missile model, autopilot design and classical altitude control system is introduced in section 2. Secondly, definition of the problem which includes motion of the platform, booster thrust vector misalignment and effect of air conditions are discussed in section 3. Then in section 4, design of the proposed controller with model prediction approach is explained and results are analyzed. Furthermore, a detailed comparison of controllers is provided for different scenarios in section 5. Lastly, a summary and conclusion are presented in section 6.

2 Missile Model and Altitude Control Design

In this study, a missile model is generated to test the performance and robustness of the proposed controller and compare it with the classical control approach. Physical and aerodynamic properties, from existing studies, are gathered to create a missile model. Furthermore, a typical acceleration autopilot is designed for the inner loop of the benchmark altitude control system.

2.1 Missile Model

Missile model architecture includes aerodynamics and inertial parameters of the missile, booster and turbojet model with an environment model. Controller commands from autopilot are also realized in the missile model. As such motion of the missile in three degrees of freedom environment will be modelled. The missile model demonstrated in Figure 1, where α is angle of attack, θ is pitch angle, γ is flight path angle, δ is deflection of control surface and $\vec{V}$ is velocity vector.

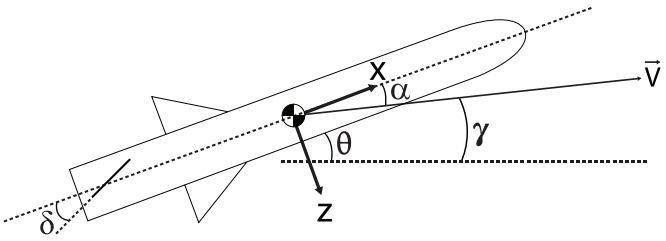

Fig. 1 Missile Model Definition.

2.1.1 Aerodynamic and Inertial Model

For the modelling of the motion and designing the controllers properly, aerodynamic and inertial properties of the selected missile are required. These parameters are taken from an existing study [14]. Inertial parameters are shown in Table 1 and aerodynamic parameters for $M = 0.8$ are shown in Table 2 and 3.

For this study, three degrees of freedom simulation environment is established. Aerodynamic stability and control derivatives are assumed to be constant for different Mach numbers. Thus, total force and moment coefficients C_z and C_m can be approximated by using equations (1) and (2). On the other

Except where otherwise noted, content of this paper is licensed under a Creative Commons Attribution 4.0 International License.

The reproduction and distribution with attribution of the entire paper or of individual pages, in electronic or printed form, including some materials under non-CC-BY 4.0 licenses is hereby granted by the respective copyright owners.

Table 1 Inertial Parameters of the Missile

m (kg)	I_{yy} (kg.m^2)	l_{ref} (m)	S_{ref} (m^2)
500	500	0.343	0.092

Table 2 Aerodynamic Stability and Control Derivatives

C_{z_α} (1/rad)	C_{z_δ} (1/rad)	C_{m_α} (1/rad)	C_{m_δ} (1/rad)
-20.5	-7.2	-24.6	-33.2

hand, axial force coefficient C_x is tabulated in Table 3 for different angles of attack values and will be interpolated throughout the simulation.

$$C_z = C_{z_\alpha} \cdot \alpha + C_{z_\delta} \cdot \delta \tag{1}$$

$$C_m = C_{m_\alpha} \cdot \alpha + C_{m_\delta} \cdot \delta \tag{2}$$

Table 3 C_x vs. Angle of Attack (α)

α (deg)	0	2	4	6	8	10	20
C_x	-0.3203	-0.3269	-0.3865	-0.4717	-0.5997	-0.7697	-2.0625

Total aerodynamic force and moment acting on missile body axes can be calculated by using equations (3), (4) and (5).

$$F^b_{x_{aero}} = Q \cdot S_{\text{ref}} \cdot C_x \tag{3}$$

$$F^b_{z_{aero}} = Q \cdot S_{\text{ref}} \cdot C_z \tag{4}$$

$$M^b_{y_{aero}} = Q \cdot S_{\text{ref}} \cdot C_m \tag{5}$$

2.1.2 Booster and Turbojet Model

Shipborne cruise missiles usually use solid-fuel rocket booster for the ballistic launch phase. It is required for the missile to gain elevation and speed so that turbojet engine can be started successfully. When impulse of the booster comes to an end, booster detaches from the missile, and ignition process of the turbojet engine starts. Solid-fuel rocket boosters burn out through a certain time with a certain propulsion. For this study, booster thrust with 45000 N of force with 3 seconds of burn out time is considered, which is valid for T_0 = 15°C sea-level temperature. For the cruise phase, Microturbo TR60 turbojet engine [15], which is a 350 daN class engine, is selected. After booster separation, windmilling process is needed for the turbojet engine to be fully operational, and this duration is assumed to be 8 seconds as it is presented in a previous study [15]. Turbojet engine will generate thrust according to the performance model in Table 4. A basic speed control loop, with speed error input and RPM (rotation per minute) command output, is also integrated into the system. As a result of this, the missile can increase its speed to the desired cruise Mach number after the boost phase.

Except where otherwise noted, content of this paper is licensed under a Creative Commons Attribution 4.0 International License.

The reproduction and distribution with attribution of the entire paper or of individual pages, in electronic or printed form, including some materials under non-CC-BY 4.0 licenses is hereby granted by the respective copyright owners.

Table 4 Turbojet RPM vs. Thrust.

RPM (%)	0	80	100
Thrust (N)	0	1000	3500

2.1.3 Control Actuator System

In this study, the autopilot produces command, δ_{com}, to the control actuation system (CAS) as a fin deflection. Since this study only focuses on the dynamics within the pitch plane, the autopilot generates commands only for the elevator. Actuator systems are driven by electrical motors, which themselves have angle and angular rate limits. As a result, elevator commands are realized through a second-order transfer function, and all parameters are given in Table 5.

$$\frac{\delta}{\delta_{com}} = \frac{\omega_{cas}^2}{s^2 + 2\zeta_{cas}\omega_{cas}s + \omega_{cas}^2} \tag{6}$$

Table 5 CAS Parameters

Parameters	Value	Unit
Natural Frequency (ω_{cas})	15	Hz
Damping Ratio (ζ_{cas})	0.8	–
Angle Limit (δ_{lim})	15	$^\circ$
Angular Rate Limit ($\dot{\delta}_{lim}$)	120	$^\circ/s$

2.2 Altitude Control Design

2.2.1 Acceleration Autopilot

There are numerous methods for designing missile pitch acceleration autopilot. Acceleration autopilot takes acceleration command, in this case a_z (acceleration at z-axis of missile body frame) and realizes this command by changing control surface (fins) deflection. For this study, typical acceleration autopilot is considered with full state feedback control structure upon the LTI (linear time invariant) system in equations (7) and (8). Whole process of linearizing the equations of motion and writing in state space form can be found in Ref. [16]. Full state feedback control will be applied on the defined state-space system. System states and control input are defined in equation (9).

$$\dot{x} = Ax + Bu \tag{7}$$

$$y = Cx + Du \tag{8}$$

$$x = \begin{bmatrix} a_z & q & \delta & \dot{\delta} \end{bmatrix}^T \quad ; \quad u = \delta_{\text{com}} = -Kx \tag{9}$$

Pole placement method is utilised to find control gain vector K. Autopilot design is performed for different design points. Dominant poles are placed such that closed loop bandwidth will be around 0.7 Hz with a damping value of 0.9. While designing the autopilot, acceleration limits for the autopilot are also decided. To do this, stability region of the missile and the maximum angle of attack limit are considered. As a result, angle of attack, α, range is selected between $[-15, 15]$ degrees. This angle of attack limit corresponds to acceleration limits in Table 6 due to the aerodynamic characteristics covered in section 2.

Except where otherwise noted, content of this paper is licensed under a Creative Commons Attribution 4.0 International License.

The reproduction and distribution with attribution of the entire paper or of individual pages, in electronic or printed form, including some materials under non-CC-BY 4.0 licenses is hereby granted by the respective copyright owners.

Table 6 Autopilot Acceleration Limit for $\alpha = 15°$

Mach Number	0.6	0.7	0.8	0.9
$a_{z_{\text{lim}}}$ (m/s)	18.01	24.52	32.02	40.53

2.2.2 Classical Altitude Control

An altitude controller is needed to generate acceleration command for the pitch acceleration autopilot. Altitude controller will be designed over the acceleration autopilot closed loop controller. Integrating vertical acceleration twice will result altitude profile of the missile given that initial conditions are known. Thus, transfer function from acceleration command to altitude can be expressed as in equation (10).

$$H(s) = \frac{h}{a_{\text{com}}} = G(s)\frac{1}{s^2} \tag{10}$$

It is concluded that acceleration autopilot is a type-0 system which means with the double integrator added to the system to obtain altitude profile, transfer function, from acceleration command to altitude as in equation (10), has now become a type-2 system. It is known that for step and ramp inputs, type-2 system is not expected to have steady-state error thus PD controller is adapted as in previous studies [5] with gains of $K_p = 0.3$ and $K_d = 0.8$.

Closed loop transfer function is expressed as in equation (11).

$$H_{cl}(s) = \frac{h}{h_{\text{com}}}(s) = \frac{K_p H(s)}{1 + K_P H(s) + sK_d H(s)} \tag{11}$$

For the ideal case scenario, initial conditions of the missile and environmental conditions are shown in Table 7. Throughout this study, altitude command will be set as 20 m.

Table 7 Nominal Simulation Conditions

h_0(m)	θ_0 (deg)	q_0 (deg/s)	θ_b (deg)	T(°C)	V_w (m/s)
10	30	0	0	15	0

In Figure 2, ideal case scenario simulation results are displayed. In Figure 2b, $a_{z_{\text{com}}}$ is acceleration command in body z-axis from benchmark PD altitude controller, $a_{z_{\text{upperlim}}}$ and $a_{z_{\text{lowerlim}}}$ are acceleration limits from autopilot design section as it shown in Table 6. The simulation starts with booster ignition and launching of the missile from a ship with an initial pitch angle. During the boost phase, which takes 3 seconds for the booster to run out, the missile gains altitude and speed. At the end of this phase, booster is separated, and pitch control starts. First, altitude controller produces positive acceleration command, in missile body axis, to turn the missile velocity vector downwards. In the meantime, the missile starts to slow down due to aerodynamic drag. After 8 seconds of windmilling and startup, the turbojet engine starts to generate thrust. The missile speeds up again while it completes its descent and performs negative acceleration pullout maneuver for transition to cruise altitude.

Except where otherwise noted, content of this paper is licensed under a Creative Commons Attribution 4.0 International License.

The reproduction and distribution with attribution of the entire paper or of individual pages, in electronic or printed form, including some materials under non-CC-BY 4.0 licenses is hereby granted by the respective copyright owners.

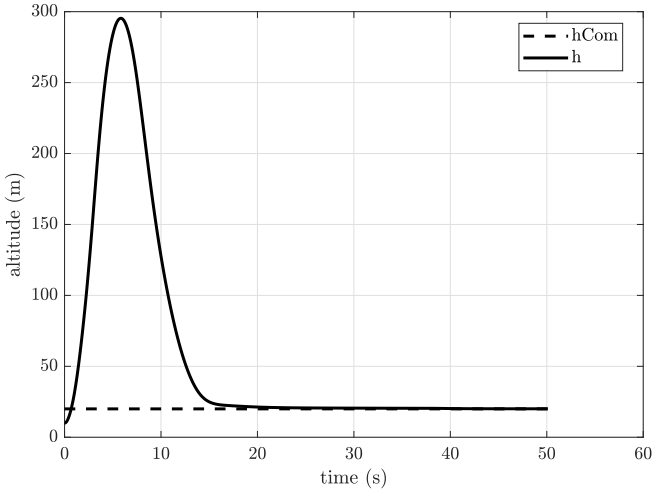

(a) Change of Altitude

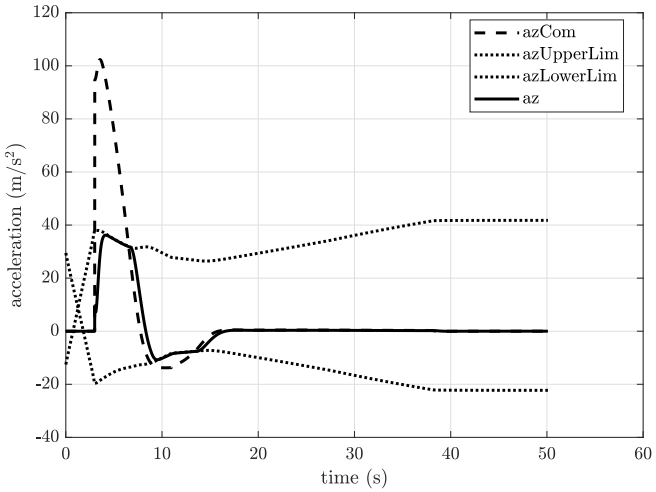

(b) Change of Acceleration, a_z with Limits and Command

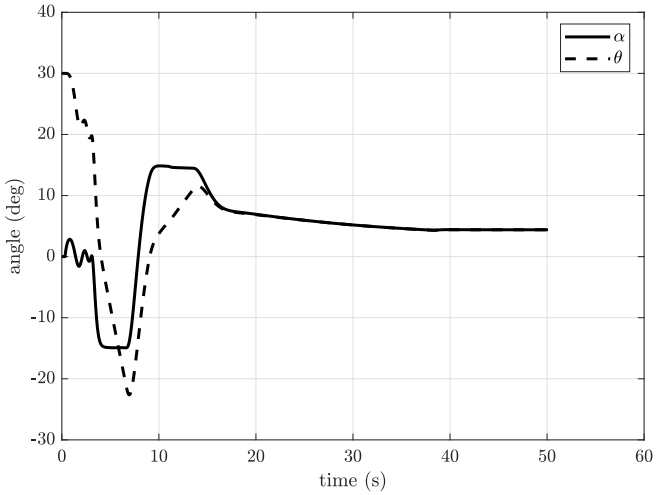

(c) Change of α and θ Angles

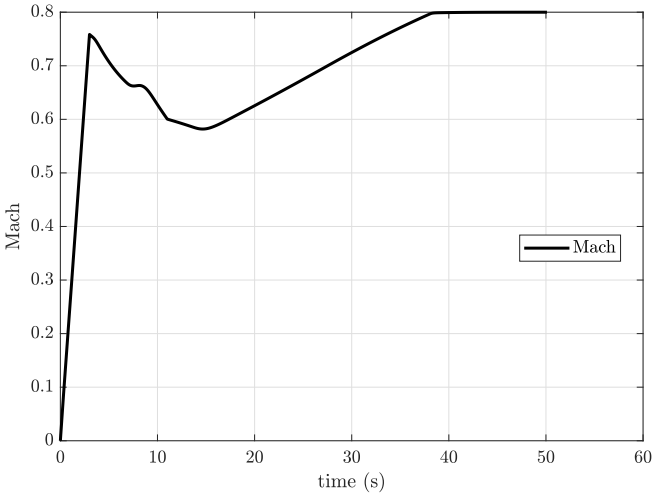

(d) Change of Mach Number

Fig. 2 Simulation Results with PD Altitude Controller with Nominal Initial Conditions.

3 Problem Definition

This section aims to introduce several significant real-world problems encountered in the domains of ship motion, the misalignment of booster thrust vectors, and effects of different environmental conditions.

3.1 Platform Motion

Initial conditions of the missile largely depend on the platform that the missile is launched from. Since the platform in the present study is a ship, its motion on the surface directly affects missile launch conditions. Especially, rough sea conditions result in large ship movements. Figure 3 displays both translational and rotational ship motions. In this study, only motion about x-axis of the ship is considered. It causes missile's launch angle θ_0 and pitch angular rate q_0 to deviate from the desired nominal condition. Standard motions of typical ships are defined in [17] for different sea states. As a challenging launch condition, sea state

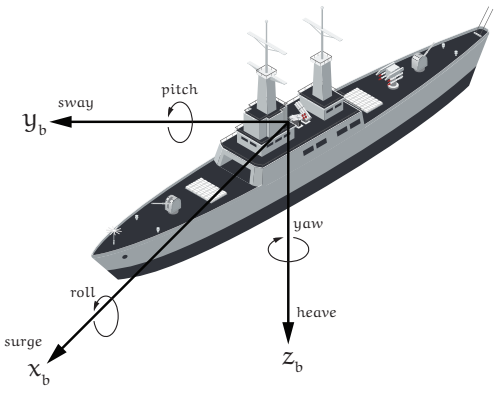

Fig. 3 Ship Principal Axes.

Except where otherwise noted, content of this paper is licensed under a Creative Commons Attribution 4.0 International License.

The reproduction and distribution with attribution of the entire paper or of individual pages, in electronic or printed form, including some materials under non-CC-BY 4.0 licenses is hereby granted by the respective copyright owners.

6 is assumed and roll motion of the platform is presumed to be ∓20 deg roll angle and ∓20 deg/s roll rate. This motion will directly affect the missile pitch motion initialization. Thus, analysis parameters happens to be as of in Table 8.

Table 8 Analysis Parameters for Platform Motion.

h_0(m)	θ_0 (deg)	q_0 (deg/s)	θ_b (deg)	T(°C)	V_w (m/s)
10	10,20,30,40,50	-20,-10,0,10,20	0	15	0

3.2 Booster Thrust Vector Misalignment

The effect of thrust vector misalignment on the missile throughout the boost phase is another major concern that can be examined. Thrust vector may be misaligned with respect to body x-axis because of assembly or production errors. θ_b is the misalignment angle of the thrust vector with the body x-axis of the missile. Maximum misalignment value is assumed as 0.3 deg. Table 9 shows the analysis parameters.

Table 9 Analysis Parameters for Booster Thrust Vector Misalignment.

h_0(m)	θ_0 (deg)	q_0 (deg/s)	θ_b (deg)	T(°C)	V_w (m/s)
10	30	0	-0.3, -0.25,...0 ... 0.25, 0.3	15	0

3.3 Effects of Different Environmental Conditions

Different environmental conditions, such as ambient temperature and wind, will be introduced, and the effects of these parameters on the propulsion system and aerodynamic parameters will be investigated. For the sake of simplicity of the analysis, the effect of wind on the sea, defined as sea states, is not considered. Thus, because of the wind or temperature, platform motion is not added to the environmental condition analyses.

Assuming that the booster's total impulse is constant, Figure 4 shows the booster profile for different ambient temperatures. It is expected since as the temperature rises, fuel in the booster burns out faster.

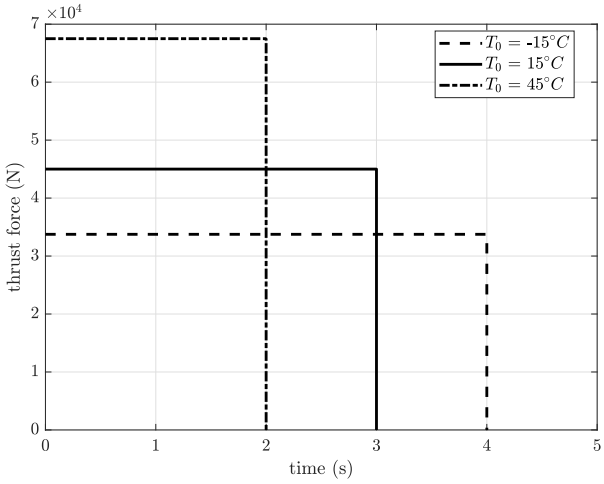

Fig. 4 Booster Thrust Profile at Different Sea-Level Ambient Temperature Conditions.

The other crucial environmental effect in the boost phase is wind. In this study, wind from two different directions and magnitudes is modeled. Knowing the air speed erroneously results in lower acceleration limits in autopilot.

Table 10 Analysis Parameters for Environmental Conditions.

h_0(m)	θ_0 (deg)	q_0 (deg/s)	θ_b (deg)	T(°C)	V_w (m/s)
10	30	0	0	-15,15,45	-20,0,20

Except where otherwise noted, content of this paper is licensed under a Creative Commons Attribution 4.0 International License.

The reproduction and distribution with attribution of the entire paper or of individual pages, in electronic or printed form, including some materials under non-CC-BY 4.0 licenses is hereby granted by the respective copyright owners.

3.4 Results of PD Method with Different Real World Problems

Figure 5 shows the simulation results when the PD method faces the real-world problems. Each run represents one of the specific problems. All results, a total of 47 simulation runs, given together in the same figure, yet analyzed separately below. Blue lines represent the nominal condition which is defined in Table 7. Black and red lines are for successful and failed runs successively.

Total of 25 conditions are simulated for the analysis of the effects of the platform motion for different initial θ_0 and q_0 values. 13 of these runs failed due to missile hitting the sea when using the PD method. For almost all of the failed runs, the missile comes from high altitudes with low Mach numbers. The PD altitude controller cannot achieve a successful pullout maneuver, and the missile ditches into the sea.

All 13 conditions are simulated to analyze the booster thrust vector misalignment for different initial θ_b values.Within these runs, 7 of them failed due to missile hitting the sea when using the PD method. Even though the root cause is different, the results are similar to the batch run results of the platform motion analysis.

A total of 9 conditions are simulated for the analysis of environmental conditions with the conditions shown in Table 10. Three of these runs failed.

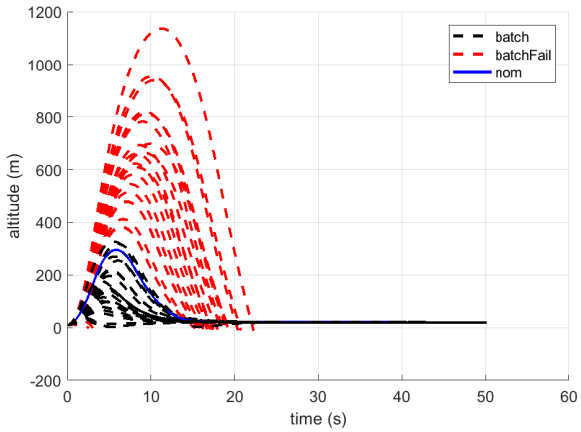

(a) Change of Altitude

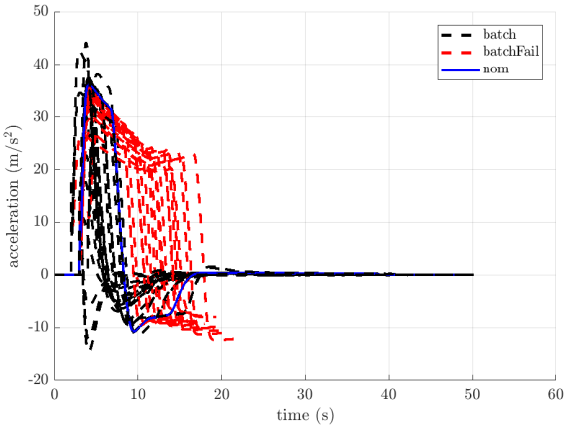

(b) Change of Acceleration, a_z

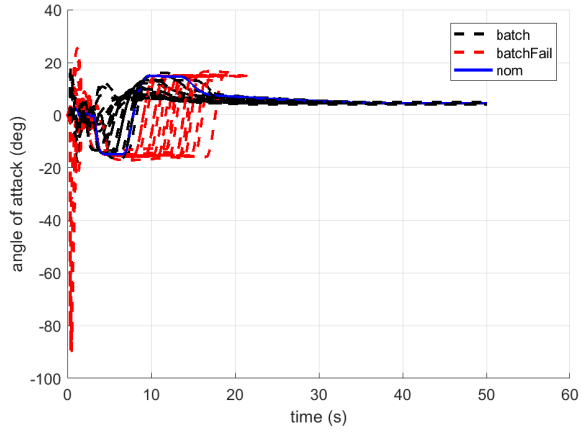

(c) Change of Angle of Attack

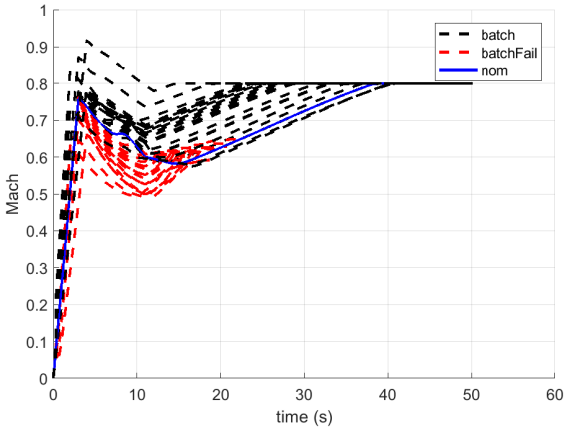

(d) Change of Mach Number

Fig. 5 Results of Different Real World Problems with the PD Method.

Except where otherwise noted, content of this paper is licensed under a Creative Commons Attribution 4.0 International License.

The reproduction and distribution with attribution of the entire paper or of individual pages, in electronic or printed form, including some materials under non-CC-BY 4.0 licenses is hereby granted by the respective copyright owners.

4 Modified PD Controller with Predictive Model

PD altitude controller can easily fail under non-ideal conditions. When the whole launch envelope is considered, a more generic and robust approach is needed. This study proposes to control, limit, and predict the dive speed using a model to predict missile states and then produce acceleration command to autopilot. If a missile can limit its dive speed at each instant according to the instantaneous conditions, it can achieve a quick but safe descent. Details of this proposed steep descent algorithm, a modified PD (MPD) altitude controller, are as follows.

Basic model to be predicted is constructed as in equation (12), where h is missile height, v is vertical speed and a is the upward acceleration. This model reflects that at any time when altitude controller commands constant acceleration a_{com}, acceleration autopilot will realize that command with a time constant τ. Thus, starting from commanding acceleration, the missile's states can be predicted at a future time with enough precision using this model.

$$\begin{bmatrix} \dot{h} \\ \dot{v} \\ \dot{a} \end{bmatrix} = \begin{bmatrix} 0 & 1 & 0 \\ 0 & 0 & 1 \\ 0 & 0 & -\tau \end{bmatrix} \begin{bmatrix} h \\ v \\ a \end{bmatrix} + \begin{bmatrix} 0 \\ 0 \\ \tau \end{bmatrix} a_{\text{com}} \tag{12}$$

The missile should dive as fast as possible for an optimum descent phase. However, it should not perform any overshoot when transitioning to commanded altitude. This is only possible with a pullout maneuver performed at the last minute with acceleration just within missile limits. With initial conditions at hand, equation (12) can be expressed in frequency domain as a set of equations. Also, by replacing a_{com} in this model with a_{uplim} and considering it as a step input, equation (13) is generated.

$$A_{\text{com}}(s) = \frac{a_{\text{uplim}}}{s} \tag{13}$$

For $t \geq 0$, solution of equation (12) as a set of equations in frequency domain can be found using inverse Laplace transform. In accordance with equation (13), using equation (14), time solution of acceleration equation is defined as in equation (15).

$$sA(s) - a_0 + \tau A(s) = \tau A_{\text{com}}(s) \tag{14}$$

$$a(t) = a_{\text{uplim}} + (a_0 - a_{\text{uplim}})e^{-\tau t} \tag{15}$$

In the same way, using equation (16), velocity solution is defined as in equation (17).

$$s^2V(s) - sv_0 - a_0 + \tau A(s) = \tau A_{\text{com}}(s) \tag{16}$$

$$v(t) = (v_0 + \frac{a_0 - a_{\text{uplim}}}{\tau}) + (a_{\text{uplim}})t + (-a_0 + a_{\text{uplim}})e^{-\tau t} \tag{17}$$

Lastly, altitude of the missile with respect to time is solved as in equation (19).

$$s^3H(s) - s^2h_0 - sv_0 - a_0 + \tau A(s) = \tau A_{\text{com}}(s) \tag{18}$$

$$h(t) = (h_0 + \frac{-a_0 + a_{\text{uplim}}}{\tau^2}) + (v_0 + \frac{a_0 - a_{\text{uplim}}}{\tau})t + (a_{\text{uplim}})\frac{t^2}{2} + (\frac{a_0 - a_{\text{uplim}}}{\tau^2})e^{-\tau t} \tag{19}$$

Except where otherwise noted, content of this paper is licensed under a Creative Commons Attribution 4.0 International License.

The reproduction and distribution with attribution of the entire paper or of individual pages, in electronic or printed form, including some materials under non-CC-BY 4.0 licenses is hereby granted by the respective copyright owners.

Initial conditions for t_0, which are a_0, v_0, h_0, are known together with the acceleration limit a_{uplim} and acceleration autopilot dynamics parameter τ is known from autopilot design. Thus, with the equations (15), (17) and (19), for $t \geq 0$, states of the system can be predicted with the assumption of missile will pull acceleration in upper limit. This model prediction is accurate enough for controller to work for the descent phase of the sea-skimming missile. Proposed MPD with prediction model is as in Figure 6.

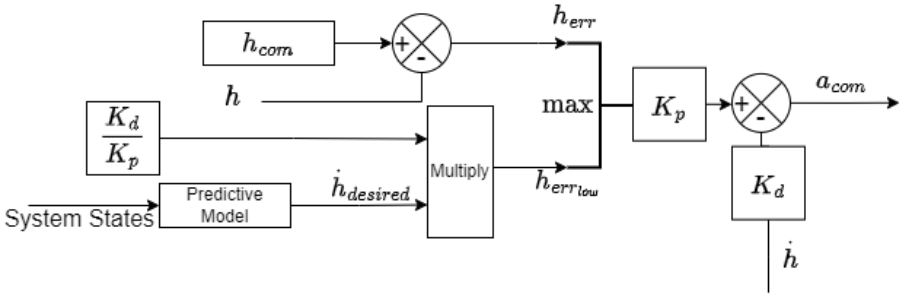

Fig. 6 Block Diagram of MPD Altitude Control System.

In Figure 7, flowchart of the proposed steep descent algorithm is shown. This flowchart explains how the proposed method works. h_{com} is already decided before missile launched from ship. Pitch control starts with separation of booster from the missile. For every time step t_i, missile states h_0, v_0, a_0 and a_{lim} are fed to the algorithm. Then, to predict the pullout time, t_p, equation (17) is solved by using Newton-Raphson method for $v(t_p) = 0$, knowing that at the end of the pullout maneuver vertical speed will be zero. If solution cannot be found in limited iteration then it can be said that missile has positive upward velocity and it will continue ascending further with this model. Hence, there is no need to limit dive speed of the missile. As a result of this, predetermined $\dot{h}_{\text{desired}}$ which is $-100\ m/s$ is set. In the case of an existence of a solution, $h(t_p)$ is calculated by using equation (19) and compared with the h_{com}. If $h(t_p)$ is not higher than the h_{com}, it means that the system has a tendency to overshoot. Thus, precautions are needed and $\dot{h}_{\text{desired}}$ is set to zero. In the case of, $h(t_p)$ is higher than the h_{com}, then optimum dive speed is calculated by using equation (20). Determining this dive speed limit is the one main outcomes of this algorithm.

Equation (19) can be defined in reverse for a certain time with the assumption of pullout maneuver ends right at the desired altitude h_{com}. Desired dive speed $\dot{h}_{\text{desired}}$ is calculated using equation (20).

$$\dot{h}_{\text{desired}} = v_0 = (h_{\text{com}} - (h_0 + \frac{-a_0 + a_{\text{uplim}}}{\tau^2}) - (a_{\text{uplim}})\frac{t_p^2}{2} - (\frac{a_0 - a_{\text{uplim}}}{\tau^2})e^{-\tau t})/t_p - (\frac{a_0 - a_{\text{uplim}}}{\tau}) \quad (20)$$

Since system only has an altitude controller and not an altitude rate controller, one way to control altitude rate is; saturating the altitude error such that proportional and derivative parts of the PD altitude controller cancels each other and set acceleration command to zero. This is achieved as follows. First of all, guidance method is defined as in equation (21). Then lower bound of the altitude error $h_{\text{err}_{\text{low}}}$ is calculated by using guidance gains and desired altitude rate as in equation (22). After that, altitude error is saturated as in equation (23). Finally, with this conscious introduction of the non-linearity, controller method is rearranged as in equation (24).

Except where otherwise noted, content of this paper is licensed under a Creative Commons Attribution 4.0 International License.

The reproduction and distribution with attribution of the entire paper or of individual pages, in electronic or printed form, including some materials under non-CC-BY 4.0 licenses is hereby granted by the respective copyright owners.

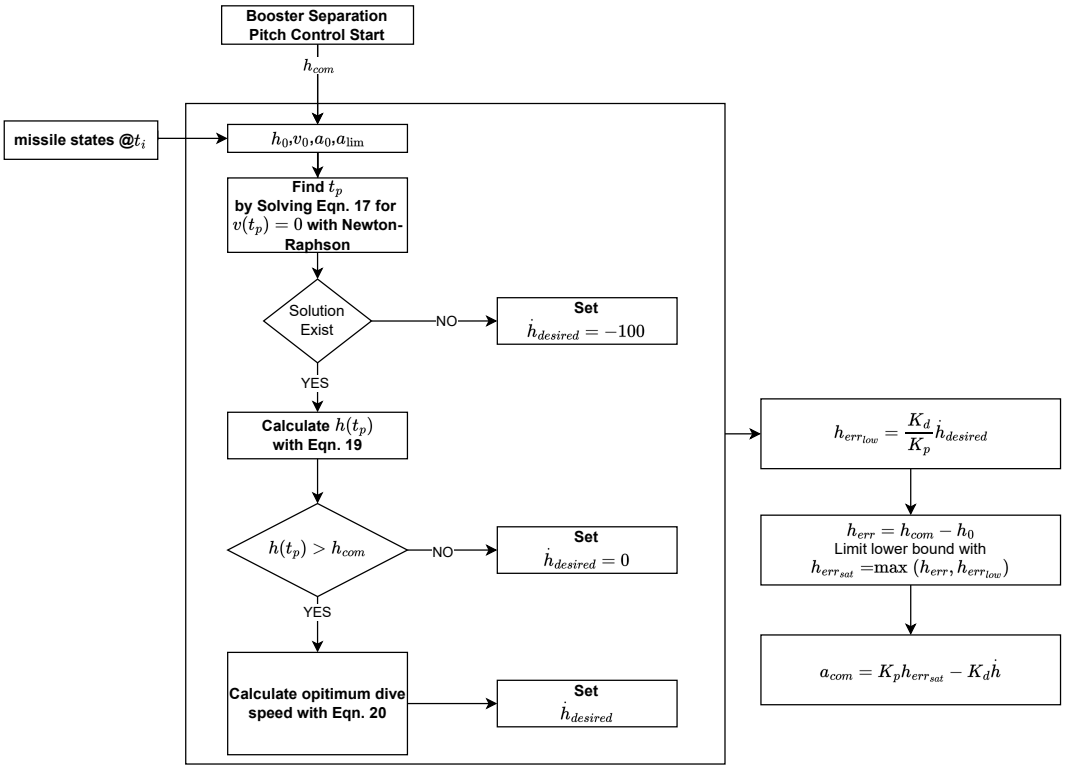

Fig. 7 Proposed steep descent algorithm's flowchart.

$$a_{\text{com}} = K_p(h_{\text{err}}) - K_d\dot{h} \quad ; \quad h_{\text{err}} = h_{\text{com}} - h_0 \tag{21}$$

$$h_{\text{err}_{\text{low}}} = \frac{K_d}{K_p}\dot{h}_{\text{desired}} \tag{22}$$

$$h_{\text{err}_{\text{sat}}} = max(h_{\text{err}}, h_{\text{err}_{\text{low}}}) \tag{23}$$

$$a_{\text{com}} = K_p h_{\text{err}_{\text{sat}}} - K_d\dot{h} \tag{24}$$

As a result, missile dive speed cannot exceed $\dot{h}_{\text{desired}}$, so the altitude rate is controlled indirectly.

5 Results and Discussion

To analyze the performance of the proposed method and compare it with the PD controller, one example condition is selected. Table 11 shows initial conditions chosen for the selected simulation. Results with benchmark PD altitude control and MPD control with predictive model can be seen in Figure 8.

Table 11 Selected Run Initial Conditions.

h_0(m)	θ_0 (deg)	q_0 (deg/s)	θ_b (deg)	T(°C)	V_w (m/s)
10	45	0	0	15	0

Except where otherwise noted, content of this paper is licensed under a Creative Commons Attribution 4.0 International License.

The reproduction and distribution with attribution of the entire paper or of individual pages, in electronic or printed form, including some materials under non-CC-BY 4.0 licenses is hereby granted by the respective copyright owners.

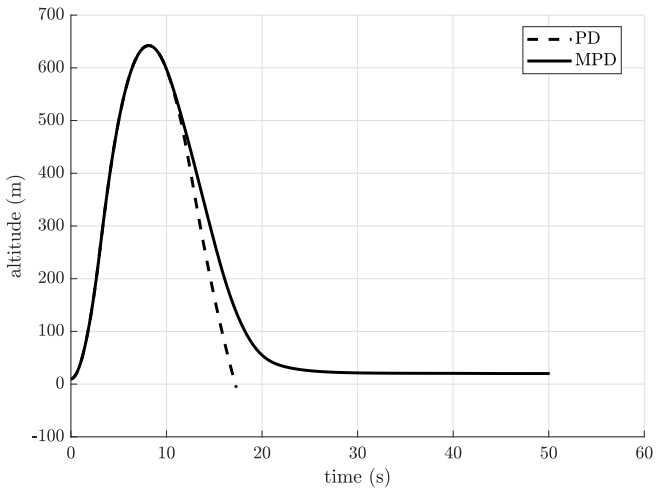

(a) Change of Altitude

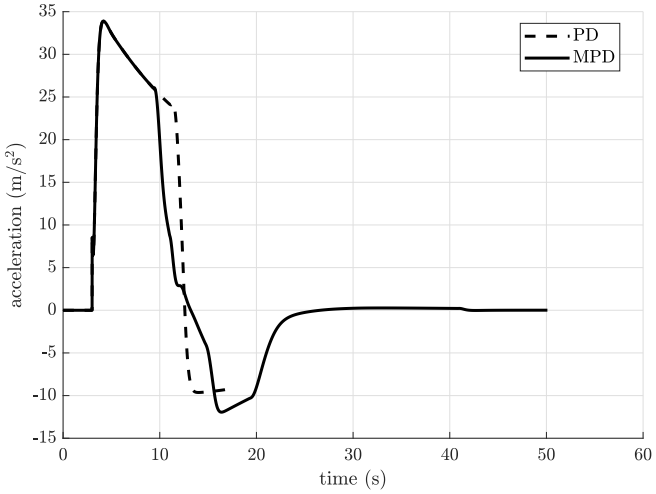

(b) Change of Acceleration, a_z

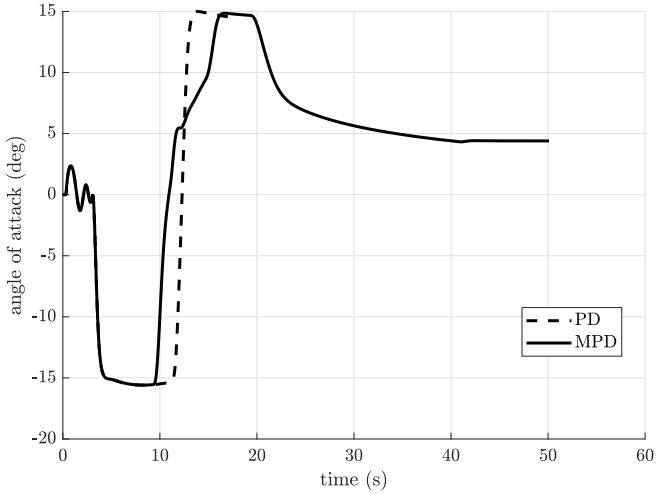

(c) Change of Angle of Attack

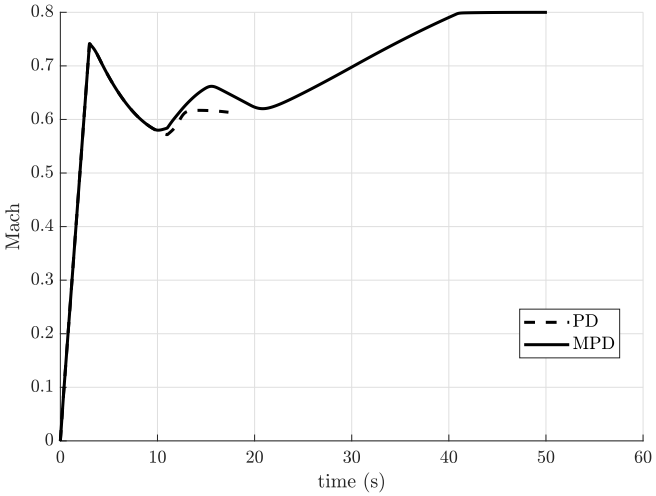

(d) Change of Mach Number

Fig. 8 Comparison of Different Control Methods.

In Figure 8, due to the high initial pitch angle, missile climbs above 600 m. At the peak altitude, both PD and MPD based guidance methods produce maximum positive acceleration commands in missile body axis. This corresponds to maximum downwards acceleration for the missile. Then, around $t = 10s$ two methods starts to differ. Because of the existence of the huge altitude error, classical controller continues to give downward acceleration command to the autopilot. In few seconds, missile vertical speed increases dangerously. Controller starts to produce negative acceleration with positive angle of attack limit at $t = 12s$ to achieve pullout. At this point missile is late for pullout and crashes into sea. On the other hand, MPD controller deliberately slows down the missile's vertical speed during the dive phase and successfully perform the pullout maneuver. In Figure 9, missile $\dot{h}$ profile for MPD controller interprets the success of the algorithm in a much clear way. During the dive phase at each instant, MPD controller decides the optimum dive speed $\dot{h}_{desired}$, calculates the error saturation limit and applies the guidance

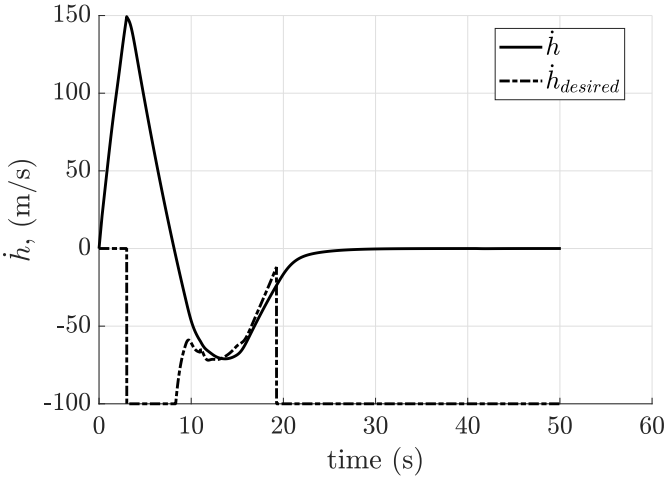

Fig. 9 MPD Altitude Control $\dot{h}$, $\dot{h}_{desired}$ Results.

Except where otherwise noted, content of this paper is licensed under a Creative Commons Attribution 4.0 International License.

The reproduction and distribution with attribution of the entire paper or of individual pages, in electronic or printed form, including some materials under non-CC-BY 4.0 licenses is hereby granted by the respective copyright owners.

method. The command-pursuit profile seen between $10 < t < 20$ seconds is the precious outcome of this algorithm which constitutes the proposed steep descent approach with MPD altitude control.

In section 3, batch simulation results of the PD altitude controller for varying non-ideal conditions were presented. These batch simulations are repeated using the MPD method, and the results are given in Figure 10. Also, success rate comparison is shown in Table 12.

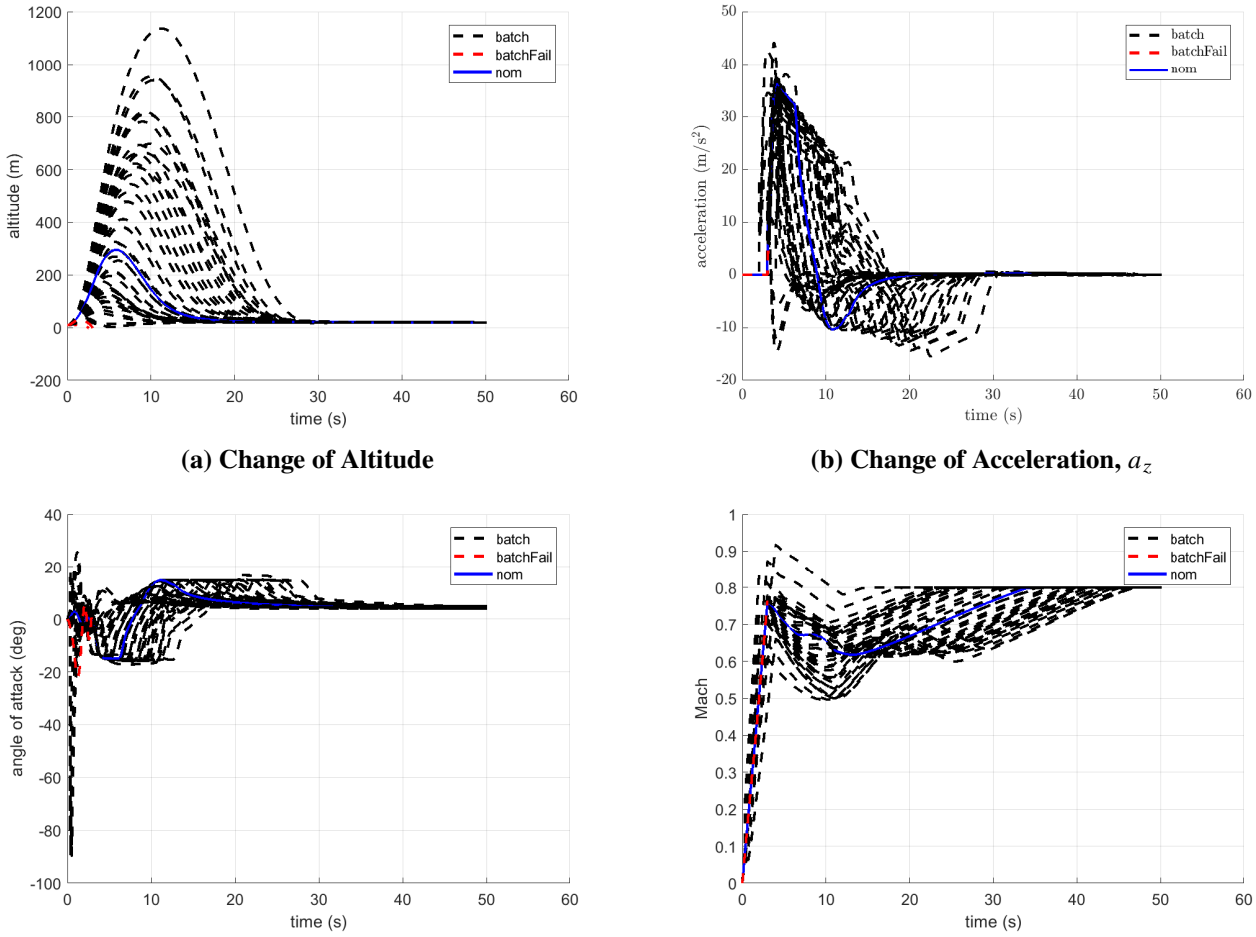

(a) Change of Altitude

(b) Change of Acceleration, a_z

(c) Change of Angle of Attack

(d) Change of Mach Number

Fig. 10 Results of Different Real World Problems with MPD Method.

Table 12 shows that for all real world problems missile encounters, the proposed method increases the success rate significantly. The benchmark method is also unsuccessful for the ones that new method is unsuccessful. This is due to the ballistic phase of the sea-skimming missile. Even before pitch control starts, the missile ditches into the sea in those unsuccessful results.

Table 12 Success Rate Comparison of Two Methods.

	PD	MPD
Platform Motion	12/25	23/25
Booster Thrust Vector Misalignment	6/13	12/13
Environmental Conditions	6/9	9/9

Except where otherwise noted, content of this paper is licensed under a Creative Commons Attribution 4.0 International License.

The reproduction and distribution with attribution of the entire paper or of individual pages, in electronic or printed form, including some materials under non-CC-BY 4.0 licenses is hereby granted by the respective copyright owners.

6 Conclusion

In this study, boost and descent phases of a shipborne cruise missile are investigated. A novel control method is proposed with MPD altitude control steep descent algorithm. The performance analysis of the proposed algorithm is done and compared with the classical altitude control approach. Rapid yet robust responses of the algorithm under varying real-world effects show that the proposed algorithm provides significant robustness to the system.

References

[1] J. Dowdle. An optimal guidance law for supersonic sea skimming. In *AIAA Guidance, Navigation and Control Conference*, Colorado, USA, 1985. DOI: 10.2514/6.1985-1866.

[2] J. Dowdle and P. Kim. Bandwidth requirements for sea skimming guidance. In *AIAA Guidance, Navigation and Control Conference*, Colorado, USA, 1985. DOI: 10.2514/6.1985-1867.

[3] Qiuqiu Wen, Qunli Xia, and Chuntao Cai. Analysis for height control-loop of cruise missile to different kinds of autopilot. In Gary Lee, editor, *Advances in Automation and Robotics, Vol. 2*, pages 507–514, Berlin, Heidelberg, 2012. Springer Berlin Heidelberg. ISBN: 978-3-642-25646-2.

[4] K. S. Priyamvada, Varghese Olikal, S. E. Talole, and S. B. Phadke. Robust height control system design for sea-skimming missiles. *Journal of Guidance, Control, and Dynamics*, 34(6):1746–1756, 2011. DOI: 10.2514/1.53577.

[5] Ozgun Dulgar, Rustu B. Gezer, and Ali T. Kutay. Extended kalman filter based robust altitude controller for sea skimming missiles. In *AIAA Guidance, Navigation, and Control Conference*, California, USA, 2016. DOI: 10.2514/6.2016-1876.

[6] S. E. Talole and S. B. Phadke. Height control system for sea-skimming missile using predictive filter. *Journal of Guidance, Control, and Dynamics*, 25(5):989–992, 2002. DOI: 10.2514/2.4977.

[7] Yin Wang and Daobo Wang. Development of an equivalent-input-disturbance based altitude controller for sea-skimming unmanned aerial vehicles. In *Proceedings of the 33rd Chinese Control Conference*, pages 151–155, 2014. DOI: 10.1109/ChiCC.2014.6896613.

[8] Ozgun Dulgar, Rustu Berk Gezer, and Ali Turker Kutay. Kalman filter based altitude control approach for sea skimming cruise missiles with sea wave adaptation. In *Proceedings of the 2019 CEAS Specialist Conference on Guidance, Navigation and Control (EuroGNC)*, Milan, Italy, Apr. 2019.

[9] Hyeonggwan Kang, Sangmin Lee, Jihoon Lee, Youdan Kim, Jinyoung Suk, and Seungkeun Kim. Altitude tracking of uav with pitch-hold constraint based on model predictive control for mine detection. In *21st International Conference on Control, Automation and Systems (ICCAS)*, pages 1955–1959, Jeju, Korea, 2021. DOI: 10.23919/ICCAS52745.2021.9649884.

[10] Koray S. Erer, Raziye Tekin, and M. Kemal Özgören. Biased proportional navigation with exponentially decaying error for impact angle control and path following. In *2016 24th Mediterranean Conference on Control and Automation (MED)*, pages 238–243, June 2016. DOI: 10.1109/MED.2016.7535911.

[11] Koray S. Erer and Raziye Tekin. Impact vector guidance. *Journal of Guidance, Control, and Dynamics*, 44(10):1892–1901, 2021. DOI: 10.2514/1.G006087.

[12] Min-Jea Tahk, Sang-Wook Shim, Seong-Min Hong, Han-Lim Choi, and Chang-Hun Lee. Impact time control based on time-to-go prediction for sea-skimming antiship missiles. *IEEE Transactions on Aerospace and Electronic Systems*, 54(4):2043–2052, 2018.

[13] Tuna Gün Aksu. Descent control algorithm design for shipborne sea-skimming missiles. Master's thesis, Middle East Technical University, 2024.

Except where otherwise noted, content of this paper is licensed under a Creative Commons Attribution 4.0 International License.

The reproduction and distribution with attribution of the entire paper or of individual pages, in electronic or printed form, including some materials under non-CC-BY 4.0 licenses is hereby granted by the respective copyright owners.

[14] Haydar Tolga Avcıoğlu. A tool for trajectory planning and performance verification of cruise missiles. Master's thesis, Middle East Technical University, 2000.

[15] Jean-Francois Rideau, Gilles Guyader, and Alain Cloarec. Microturbo families of turbojet engine for missiles and uav's from the tr60 to the new bypass turbojet engine generation. In *44th AIAA/ASME/SAE/ASEE Joint Propulsion Conference & Exhibit*, Connecticut, USA, 2008. DOI: 10.2514/6.2008-4590.

[16] Ozgun Dülgar. A robust altitude control approach for sea skimming missiles. Master's thesis, Middle East Technical University, 2018.

[17] Dept. of Defense United States. Interface standard for shipboard systems, section 301a, ship motion and attitude. *Millitary Standards*, July 1986.

Except where otherwise noted, content of this paper is licensed under a Creative Commons Attribution 4.0 International License.

The reproduction and distribution with attribution of the entire paper or of individual pages, in electronic or printed form, including some materials under non-CC-BY 4.0 licenses is hereby granted by the respective copyright owners.